Analysis of the rooftop photovoltaic potential in a real case: Energy community of the music school in Adeje

Master Thesis

Author: Miguel Marrero Oñate

Advisors: Ricardo Guerrero Lemus,

Luis Hernandez Salmeron,

Iñigo Berazaluce Minondo

September 7, 2022

Foreword

The idea and need of this Master Thesis originates from an innovation project (AdejeVerde) that is being carried out jointly by EnergyRIS, a spin-off from the University of La Laguna and E.ON Group Innovation GmbH. During the last semester of the Master's course, I did my curricular internship in the latter company, specifically in the Energy Communities and Networks domain, where I mainly worked on the AdejeVerde project. The project consist primarily of creating local energy communities by offering photovoltaic installations to buildings with available roof space and linking these prosumers with consumers in the vicinity, which benefit from the photovoltaic generated electricity through self-consumption.

The first local energy community created within the scope of this project was in the area of the music school of Adeje, a municipality in the island of Tenerife (Spain). The 99kWp photovoltaic installation on the rooftop of said building will supply the music school itself, as well as neighbours and commercial premises within a radius of 500m, with renewable energy for self-consumption, forming the biggest energy community in Spain according to the number of participants.

Since the project aims to install a substantial amount of photovoltaic installations in the residential sector to foster the creation of energy communities and energy self-consumption, a major concern that arises is how this may impact the distribution grid. The topic of this Master Thesis comes from the need to analyse the impact of a large scale deployment of photovoltaic installations in condensed residential areas in a real case scenario.

Miguel Marrero Oñate

Notice of use

This Master thesis makes use of confidential information obtained from the local distribution company EDISTRIBUCIÓN Redes Digitales, S.L.U. As such, figures received from this source that are not open to the public domain will be omitted in the non-private version of this thesis.

Abstract

Rooftop photovoltaic emerges as an essential resource to promote the energy transition. It opens up the possibility to create energy communities and share the generated electricity within a neighbourhood, aiding to confront the energy crisis. However, low voltage distribution grids where originally designed radially, with a mainly one-directional power flow in mind. As such, a high penetration of distributed generation such as rooftop photovoltaic will negatively impact the grid, increasing the voltage profile and causing reverse power-flows. Thus, it is key to determine the limits set by the applicable regulation and analyze the effects of rooftop photovoltaic on the grid performance.

This work aims to determine the impact on the distribution grid of an intense deployment of rooftop photovoltaic in a real case scenario, the surroundings of the music school in Adeje, Tenerife (Spain). For this purpose, the current statutory limits, as well as the network topology, the rooftop area and real consumption data of the vicinity are taken into account. A simulation is performed using the software OpenDSS, and the influence on the grid is estimated for different penetration scenarios. The results show that the transformer capacity limitation allows the integration of 420kWp. Setting this limitation aside, this value could be increased up to 579kWp without surpassing voltage limits, while the maximum photovoltaic potential in the vicinity according to available rooftop area is estimated at 1859,21kWp, but it would breach the current grid codes. To allow higher penetration limits, solutions such as the Volt-Var and Volt-Watt techniques as well as distribution static synchronous compensators are required.

Acronyms and abbreviations

AC	Alternate current	**MPPT**	Maximum-power-point tracking
DC	Direct current	**MV**	Medium voltage
DG	Distribution generator	**OpenDSS**	Open Distribution System Simulator
EMMA	Adeje Municipal Music School	**PCC**	Point of common coupling
EPRI	Electrical Power Research Institute	**PNIEC**	National Integrated Energy and Climate Plan
EU	European Union	**PV**	Photovoltaic
HV	High voltage	**PVGIS**	Photovoltaic Geographical Information System
IEA	International Energy Agency	**RES**	Renewable energy source
IRENA	International Renewable Energy Agency	**TMY**	Typical meteorological year
LV	Low voltage		

Contents

List of Figures

1 Introduction

Distributed photovoltaic (PV) generation prevails as an essential tool to tackle the global energy and climate crisis. In 2021, the European Union (EU) updated its goal of reducing the greenhouse gas emissions up to 55% with regard to the levels of 1990, following the compromise of the 2015 Paris Agreement and its limitation of a 1,5°C temperature rise [8]. In Spain, the National Integrated Energy and Climate Plan (PNIEC) [9], establishes the following objectives for 2030 to meet the targets of the Paris Agreement and reach climate neutrality by 2050: 23% reduction of greenhouse gas emissions, 42% renewable energy sources (RES) in energy end use, 74% electricity generation from RES and the installation of 59 GW RES capacity. From among all renewable energy technologies, PV has not only been prevalent for many years, but is expected to experience the highest growth, multiplying its 2018 global installed capacity (480 GW) by eighteen by the year 2050 (8519 GW), as stated by IRENA [10] and shown in Figure 1.

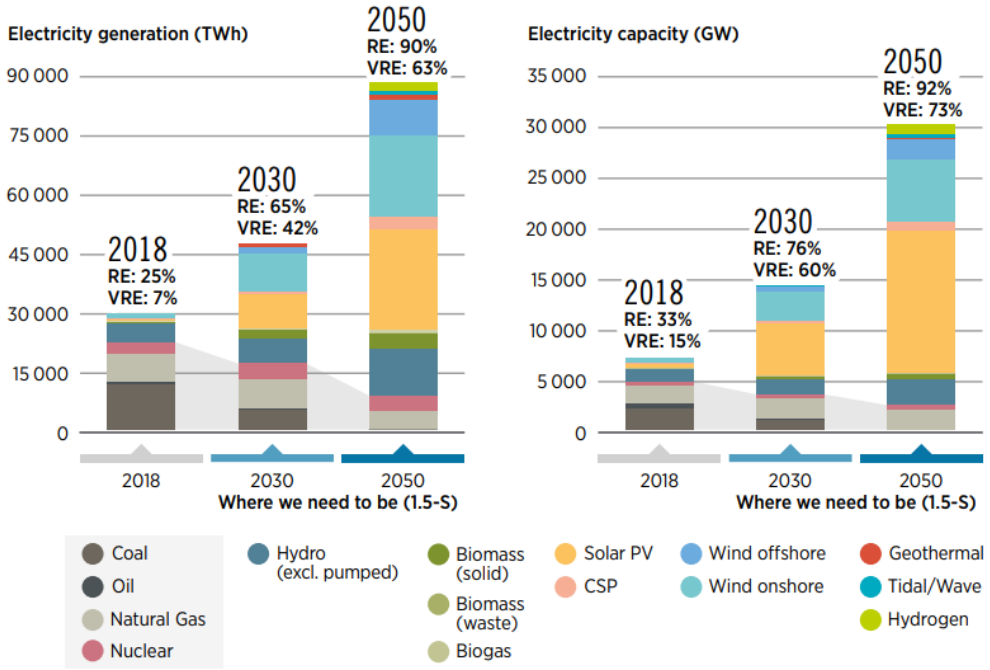

Figure 1: RES installed capacity following the 1,5°C scenario, extracted from [1].

Furthermore, IRENA predicts that by 2050, 40% of total PV capacity would be distributed, meaning that it would not be located in large generation plants connected to the medium- (MV) or high-voltage (HV) grid, but it would rather consist of many dispersed PV installations mainly located at the MV or low-voltage (LV) grid. Several countries worldwide already display high rates of distributed PV: 70% of current PV capacity in Germany is installed in the LV grids, while this number goes up to 98% in the case of Italy [11].

This decentralised PV electricity generation arises as a solution to confront the energy crisis. By generating electricity closer to the consumers, power losses and

congestion in the grid are reduced. Furthermore, distributed PV generation offers residential consumers the possibility to install PV on their own rooftops, thus becoming prosumers, allowing them to benefit from the generated electricity [12]. According to IEA [13], there are currently around 25 million rooftop PV installations worldwide, and this value is expected to reach 240 million by 2050. Hawaii and Australia are among the biggest contributors. The latter closed last year with 10 GW of total installed rooftop PV capacity [14] and the amount of single-family houses with rooftop PV at their disposal in Oahu, Maui County and Hawaii Island were 36%, 29% and 21%, respectively [15]. Moreover, to further incentivise self-consumption from rooftop PV, an energy community may be established, so that the prosumer is able to share the generated electricity with its neighbours. This figure is defined in the Directives (EU) 2018/2001 [16] and 2018/944 [17], as a congregation of citizens and local authorities to collectively participate in renewable energy projects. The European Commission estimates that by 2050, around 37% of EU households would participate in energy communities [18]. However, the Canary Islands have still major room for improvement in this matter, from 3.800 PV self-consumption installations, only 22 are in a collective scheme [19].

Self-consumption of PV energy will aid residential consumers meet the increase in residential energy demand, which is expected to double by 2050 [13], foster the emergence of electric vehicles [20] and allow citizens to confront the current exceptionally high retail electricity prices [21]. Despite this, an intense deployment of residential PV will negatively influence the distribution, and to some extent, the transmission grids, which were originally conceived to transmit electricity from large power plants in the HV or MV grids to consumers located at the LV level. Voltage variation and thermal limits of components are the most common limiting factors. Thus, large-scale implementation of rooftop PV would require to firstly analyse the available capacity of the grid and the probability to surpass grid code limits, thus determining if grid reinforcement is necessary.

The aim of this work is to determine the impact on the distribution grid of an intense deployment of rooftop PV in a real case scenario, the surroundings of the music school in Adeje, Tenerife (Spain). Tenerife is an isolated grid, and it mainly depends on the import of fossil fuels for its energy generation, although its conditions for RES are very favourable, especially rooftop PV due to high solar radiation and predominant areas of flat rooftops. That is why it is essential to study the viability of its large-scale implementation, locate potential limiting factors affecting the grid infrastructure and propose amendments required for the energy transition.

This work is structured as follows: In Section 2 the existing literature regarding PV deployment at the distribution grid is reviewed and the statutory grid code limits are presented. In Section 3 a simulation will be performed using the software OpenDSS, while the grid topology, the rooftop area and real consumption data of the vicinity will be taken into account. The influence on the grid will be estimated in Section 4, while in Section 5 the results are discussed and compared with other analysis from the literature and possible solutions are proposed. Finally, Section 6 concludes this work and proposes future lines of research.

2 Theoretical framework

2.1 Grid-connected PV

PV systems generate electric energy from incident solar radiation through the photoelectric effect. The main environmental parameters affecting the PV electricity production are the ambient temperature and the irradiation. As seen on Figure 2, the higher the irradiation on the PV system, the higher the output power. It is noteworthy that the short-circuit current I_{SC} increases proportionally, while the open-circuit voltage V_{OC} is barely affected by the irradiation.

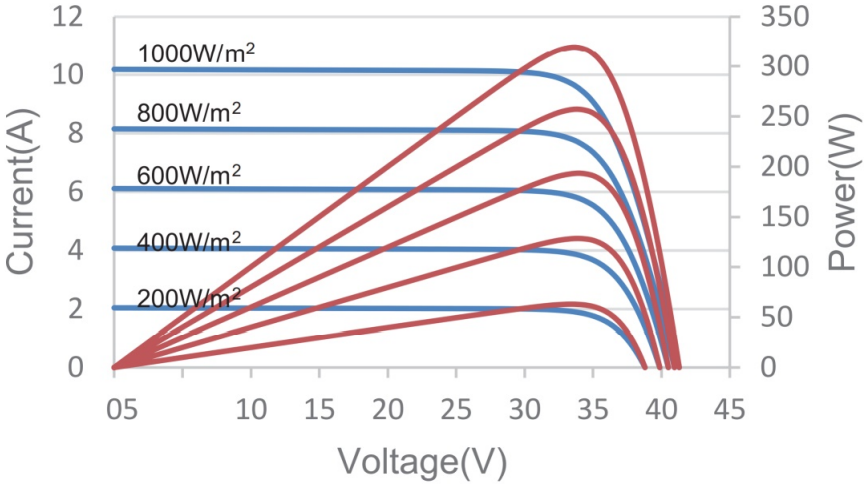

Figure 2: Effects of irradiation on PV performance.

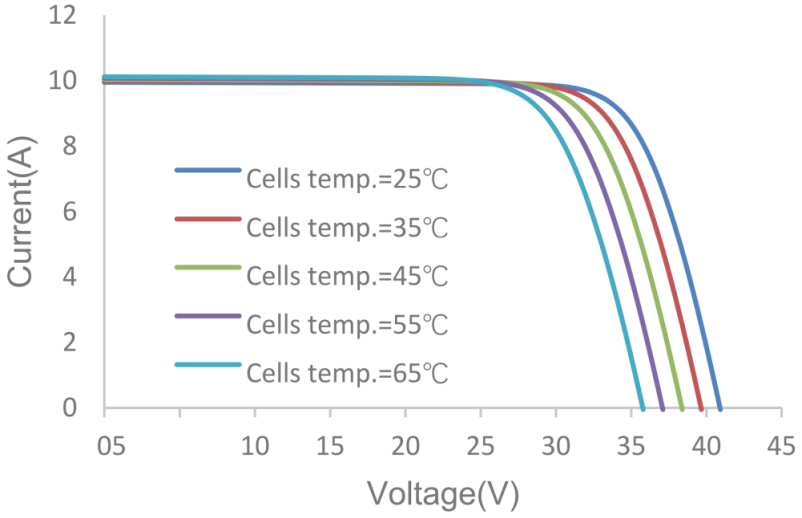

Figure 3: Effects of temperature on PV performance.

Moreover, Figure 3 reflects the effect of the cell temperature on the PV system's output. In contrast to the irradiation parameter, I_{SC} stays nearly unchanged for dif-

ferent temperatures, while V_{OC} decreases with increasing temperatures. Therefore, the PV output power decreases with higher temperatures.

The rooftop PV systems studied in this work follow the typical structure shown in Figure 4. These grid-connected PV systems consist of PV modules installed on residential rooftops, connected to an electric power converter: a DC/DC converter with Maximum Power-Point Tracking (MPPT) followed by a DC/AC converter, also known as inverter. Usually, the inverter already incorporates the MPPT functionalities, which consist of changing the operational point along the U-I curve of the PV modules to reach the point with the highest power output. Additionally, the inverter converts DC power to AC power, while providing filtering and safety features. The AC power reaches the main distribution panel, from where it can either be self-consumed by the local loads or, in its absence, be exported to the electrical grid.

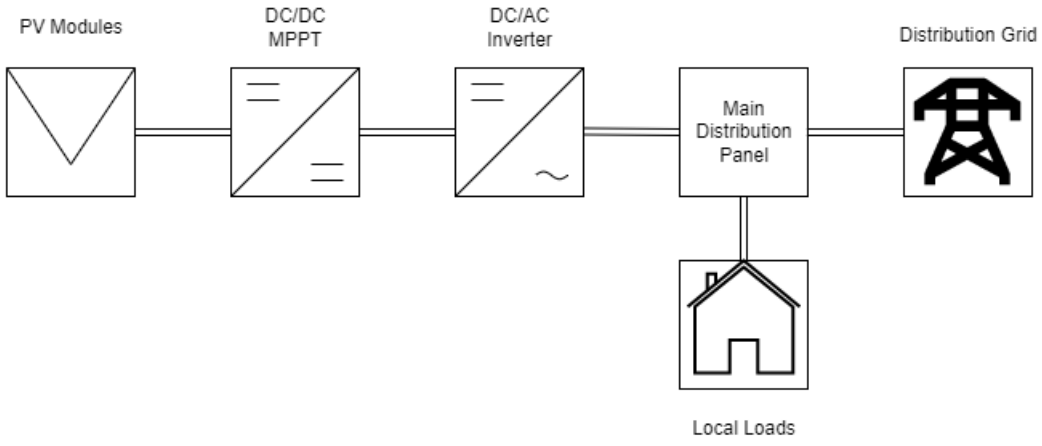

Figure 4: Block diagram of a grid-connected PV system.

PV hosting capacity is a term used to define the maximum PV generation capacity that can be connected to a grid section without breaking any grid code or legislation. Traditionally, the electricity grid was conceived with a one-directional power-flow in mind, from generating power plants at the HV and MV levels to the consumers at the LV level. Furthermore, distribution networks at the MV and LV levels are usually operated radially, meaning that the electric energy flows from the main substation to the transformer stations, and from there to the different consumers through the respective points of common coupling (PCC). Hence, the PV hosting capacity tends to be restricted to avoid impacts on grid operation and reliability, caused from the redeployment of active and reactive power flows [22].

As can often be found in the literature, a key factor delimiting PV hosting capacity is grid voltage deviation. Figure 5 illustrates the grid equivalent circuit from a general generator point of view. For a fixed grid voltage, the voltage variation in the system will vary according to the grid impedance (X, R) and the generator voltage, which will in turn depend on the injected active and reactive power.

An approximation for the calculated voltage deviation can be found in Equation

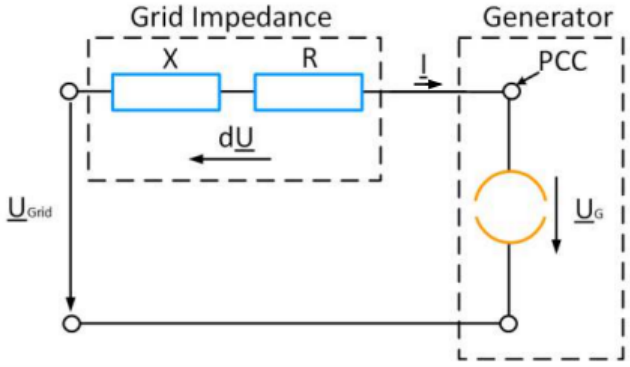

Figure 5: Equivalent circuit of a grid-connected generator, extracted from [2].

1. It can be extracted that, for a fixed grid voltage, the principal factors affecting the deviation are the grid impedance and the injected active and reactive power by the generator, as stated above. It is relevant to note that while higher active power injection will always cause a voltage increase, the reactive power injection may also decrease it. In fact, underexcited operation (negative Q) will reduce the voltage while overexcited operation will increase it [2]. In addition to this, in Equation 2 it can be identified that, for a certain generator phase angle ϕ, and therefore, a specific power factor, the R/X characteristics of the grid is the main influencing parameter. With a large R/X value a higher compensation through reactive power will be required to maintain an acceptable voltage level.

$$dU \approx \frac{(R * P) + (\mp Q * X)}{(U_{Grid})^2} \tag{1}$$

$$dU \approx \frac{R * P}{(U_{Grid})^2} * [1 + tan(\phi) * \frac{1}{R/X}] \tag{2}$$

In relation to this, Figure 6 illustrates a schematic of a distribution generator (DG) and a local load connected to the grid via a PCC, a LV line and a transformer station, as well as the impact of the DG's active and reactive power, respectively, on the LV line voltage. The load will consume active power causing a voltage drop and it may inject or absorb reactive power depending on its inductive or capacitive nature. In opposition to this, the DG will inject active power, producing a voltage increase in the line. Additionally, some DGs, as is the case with PV systems' inverters, may be able to control their reactive power output, increasing or reducing the line's voltage accordingly [2].

Traditionally, distribution voltages have been regulated through on-load tap-changing transformers, or so called voltage regulators, and capacitor banks [23]. Despite its common use over the last decades, capacitor banks have shown to lack the needed flexibility, operating in restrictive discrete steps, while voltage regulators are limited to only sense the secondary voltage, missing potential issues further along the feeder. This justifies the need for innovative grid voltage control techniques.

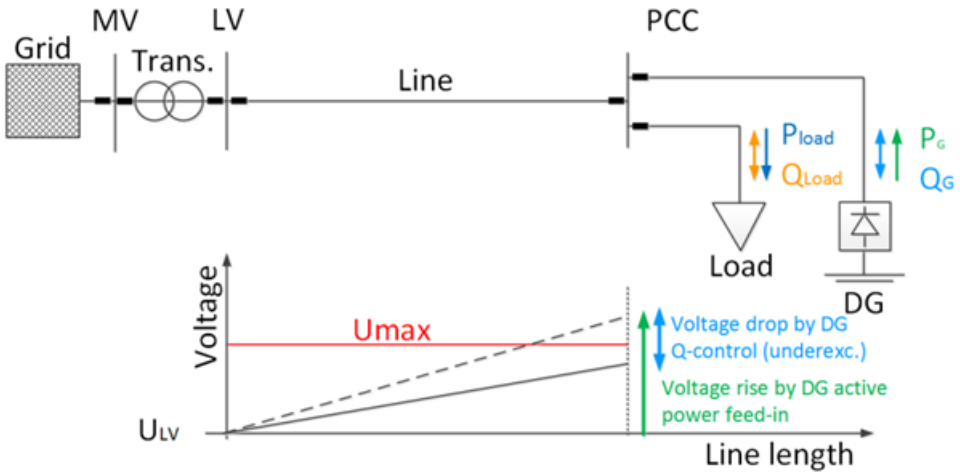

Figure 6: Block diagramm and voltage deviation of a grid connected distribution generator, extracted from [2].

The European Standard prEN50549-10, which is still in its draft state, defines that PV inverters shall be capable of providing grid voltage support through Volt-Var and Volt-Watt techniques. As shown in Figure 7a), in the Volt-Var technique, whenever the grid voltage exceeds the limits of the voltage band, the PV inverter will enter in capacitive or inductive operation, injecting or absorbing, correspondingly, reactive power at a constant rate, until either the voltage is readjusted or the voltage limits of the inverter are reached. Since no active power is curtailed, allowing to take full advantage of the PV generation, this technique seems to be the most cost-effective for the prosumer. However, it requires flexible power factors to be permitted, and it may lead to over-heating of grid assets due to the increased current flows [3].

Figure 7b) illustrates the Volt-Watt technique, for which in case of an overvoltage, the inverter will reduce the active power output at a constant rate until the voltage is corrected to be within statutory limits or the inverter reaches its limit for continuous operation. While this technique requires active power to be curtailed, it can be easily implemented by adjusting the inverter's control scheme [3].

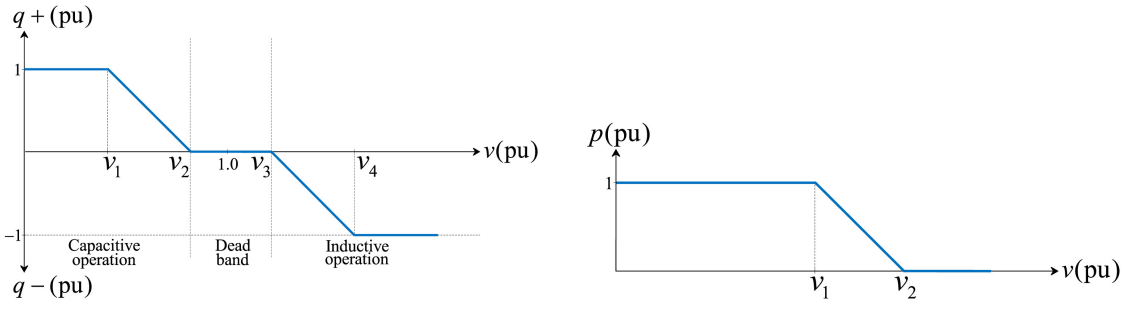

(a) Volt-var technique

(b) Volt-watt technique

Figure 7: Volt-Var and Volt-Watt technique, extracted from [3].

2.2 Literature review

It is expected that, in the near future, PV systems will contribute to grid stability and reliability by providing ancillary services through the inverter, such as congestion management, frequency, and voltage control through active and reactive power compensation [2][24][25]. For this purpose, a widespread IT-communication infrastructure needs to be developed, to apply centralized as well as decentralized control structures and allow its interaction. For example, German distribution system operators apply local voltage control for DG systems, whose characteristics are configured by a central controller, enabling fast responses and higher power quality [2].

However, a major concern regarding the Volt-Watt technique for grid voltage control is its unfairness towards users, benefiting those with a PCC located near a transformer station. The further away the PCC is from the station, the higher the power curtailment needed to maintain the voltage at a permissible level. This is why the German Renewable Energy Source Act (EEG 2014 §9) sets a fixed power limitation of 70% of the installed capacity to PV systems below 30 kWp without a distribution system operator remote interface. Although this limitation avoids unfairness among users' locations, this causes power curtailment also when no grid voltage regulation is needed. As a countermeasure, [2] analyses 17 German real case scenarios and proposes reactive power control (Volt-Var technique) to raise PV hosting capacity, up to a median of 70%-90%. Appropriately set reactive power strategies would allow to support grid voltage without major grid losses or the need for reactive power compensators. An additional remark is raised in [24], stating that reactive power variation in LV grids may have a lesser contribution due to its high R/X value. In spite of this, it is favoured over active power curtailment to avoid economic losses.

A general modification of grid standards to permit PV systems to contribute to grid power compensation would be essential according to [25]. PV systems would support in reactive and active power control, the latter would also allow grid frequency control. It is stated that a widespread integration of actively controlled, multifunctional PV systems would allow their limitless integration into the grid. This level of integration is usually called PV penetration, and is defined differently depending on the source. The most common definitions for PV penetration into a grid are:

- relation of installed PV capacity to the transformer capacity
- relation of installed PV capacity to the feeder minimum/maximum load
- ratio of installed PV capacity to the minimum active power load
- ratio of annually generated PV energy to total consumption
- ratio of roof space occupied with PV installations to total roofspace

The first three listed definitions are the most extended. Furthermore, PV penetration based on transformer capacity is widely adopted from many distribution network service providers [26]. Although this definition is better suited for power or current flows, it fails to represent impacts on grid voltage. Hence, a parallel analysis of voltage variation would be required [27].

The studies performed in [27],[28],[3] and [29] conclude that the disposition of PV systems along the feeder plays a crucial role in PV penetration. A scenario with evenly distributed PV systems along the feeder will prove to reach higher penetration limits than a scenario in which the majority of PV systems are installed concentrated at specific points of the feeder. Despite this, for small PV systems, the PCC at the building connection point is considered the most economical. Furthermore, the location in relation to the transformer station is crucial, since the penetration level increases the closer the PV systems are to the station. In fact, the limiting factor varies according to the distance, since PV connected to short LV lines will rather be restricted by conductor current capacity, while longer distances will be limited by voltage problems. In the end, the studies agree that the general limiting factor tends to be the voltage profile of the feeder. It is concluded in [3] that the harmonic distortion of PV systems is negligible, and while [30] indicates that islanding would not be a technical restriction for widespread PV penetration, a unity inverter power factor is recommended.

The study in [29] identifies that in an optimal regular distribution of PV systems, the surplus PV power flows reversed to the substation without surpassing its capacity and that PV penetration is limited by average minimum load on the feeder. Further restraining factors found in [31] are the feeder length and impedance, as well as the impedance of the transformer station. This last study highlights the importance of analysing the most delimiting scenarios when determining PV hosting capacity, those being the early night hours when energy consumption reaches its peak and PV generation is low or absent, causing undervoltages in the line, as well as midday hours, when PV generation usually reaches its maximum and consumption tends to be rather low, producing overvoltages.

The studies performed in [32] and [21] aim to determine the potential of rooftop PV in Europe. While the first concludes that if all available rooftop area would be utilised, up to 1500 TWh of annual electricity generation could be reached from PV systems (using a conservative ratio of $1kW/7m^2$), the second delimits the result further down to 680 TWh, calculating the technical potential through a combination of satellite and statistical data with machine learning. This lower value would already represent a 25% of current electricity consumption generated from rooftop PV. This latter study also mentions that in order to achieve said levels of PV penetration, the implementation of grid voltage support techniques through smart inverters would be essential to increase in up to 40% the installed PV capacity, upgrades of the grid infrastructure would also be required to further increase the PV penetration, contrasting the statement found in [25].

2.3 Legal framework

The analysis performed in this work is based on a real case scenario located in Adeje (Spain), thus, it is fundamental to state the applicable regulation and statutory grid limits.

Firstly, the Royal Decree 244/2019 [12] opens up the possibility to grid-connected PV self-consumption, and defines the different schemes of self-consumption, as well as the respective technical grid connection and economical compensation. Furthermore, the Directive (EU) 2019/944 [17] states in Article 32, that European State members shall provide a regulatory framework to promote that distribution system operators receive ancillary services from DG to support grid stability and allow the development and efficient exploitation of the distribution grid. These ancillary services shall be provided in a fair and transparent procedure, based on the requirements of the electricity market. In relation to this, the recent Royal Decree-law 6/2022 [33] obliges electricity distribution companies to include in their next years investment plans actions aimed at increasing the distribution grid hosting capacity, prioritizing areas with a high concentration of RES.

On the subject of statutory grid limits, the European Standard EN 50160 defines the voltage limits for LV grids at 230V +/- 10%. At a national scale, while the Spanish Low Voltage Electrotechnical Regulation [34] states that the maximum permissible voltage drop in the mains cable of a distribution feeder would be determined by the respective distribution company, the Royal Decree 1699/2011 [35] establishes that the contribution of a DG to the voltage deviation in a distribution line should not exceed 2,5% of the line's nominal voltage. It also limits the injected energy's power factor to 0,98 when the DG exceeds 25% of its nominal power. Moreover, it determines that when a DG is connected to a building's internal grid, such as the main distribution panel, the consumers contracted power needs to be increased to match the installed PV capacity. Lastly, the Circular Letter 1/2021 of the National Commission for Markets and Competition [36] sets the ratio of injected DG power to 50% of the distribution line capacity as well as the transformer station capacity for the respective voltage level. However, in case of grids with voltage levels below 36 kV, this value is set to 70%.

This work aims to, in the first step, simulate a LV distribution grid representative of the neighbourhood of the municipal music school in Adeje (EMMA), based on real grid topology and consumption data. As a next step, the maximum PV installed capacity will be determined, complying with current Spanish grid codes. As such, it represents a practical real-case testing scenario to determine the effects of high PV penetration, and its limiting factors in the current regulations, justifying the relevance of this work. Finally, the impact of the integration of the maximum PV potential according to the available roof-space will be tested, and potential solutions will be proposed to promote the integration of rooftop PV.

3 Methodology

The LV distribution grid of the EMMA is simulated using the Open Distribution System Simulator (OpenDSS) [37] V9.4.1.2. It is a free, open-source electrical system simulation tool provided by the Electrical Power Research Institute (EPRI) for utility distribution systems. In this work, the stand-alone executable version is used through a text-based user interface. The program is executed to perform a yearly time-series simulation including a LV grid modelling based on the actual distribution grid, real residential loads and real PV systems' parameters, such as ambient temperature, solar irradiation and PV as well as inverter specifications. This distribution grid modelling is indicatively represented in Figure 8, as a simplified version containing only a single bus.

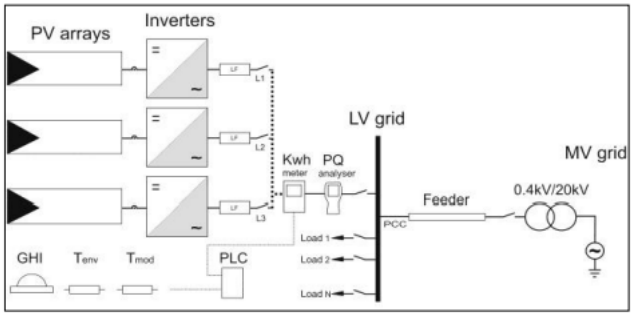

Figure 8: Indicative block-diagram of the LV grid modelling in OpenDSS, extracted from [4].

As an additional reference to model the different parameters, the test circuits provided by EPRI were used, namely the European-LV-Test-Feeder as well as the Ckt-5 test circuit provided as an example.

3.1 Grid parameters

3.1.1 Topology

To accurately model the EMMA's grid topology, real data was obtained from two private sources, in addition to public available grid information. Firstly, a detailed map of the electrical network was requested from *Inkolan* [5], a partnership association made up of most of the major utility operators in Spain, providing information related to the electricity, water and gas infrastructures. In the obtained map represented in Figure 9 it can be recognized that the EMMA (marked with a red dot) is connected to a transformer station placed in the park to the north. This transformer station supplies most of the residential blocks located at the north-north-east of the EMMA. The green line represents the LV grid (230/400V), while the blue line represents the MV grid (20kV).

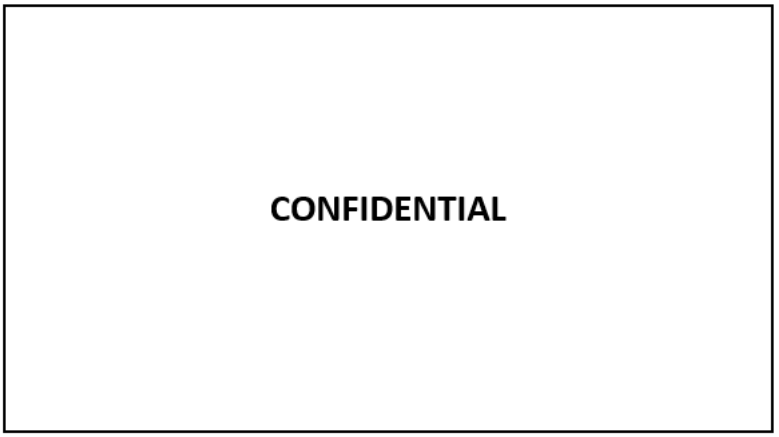

Figure 9: Detailed map of the electrical grid infrastructure, obtained from *Inkolan* [5].

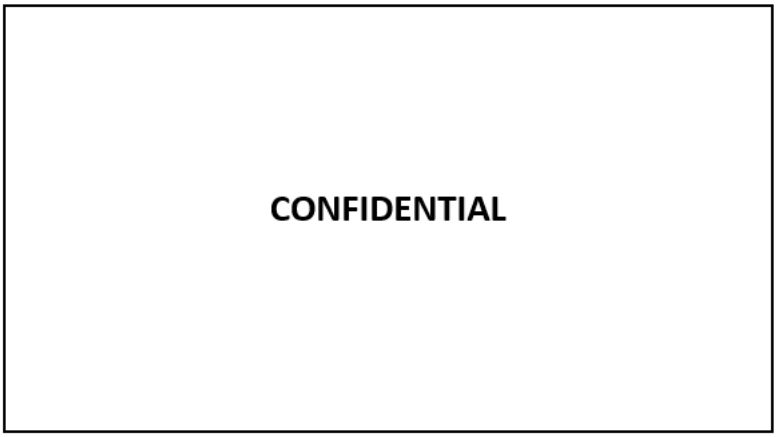

Figure 10: Transformer stations located in the 500m area of the EMMA, obtained from *e-distribución* [6].

Secondly, EDISTRIBUCIÓN Redes Digitales, S.L.U. (e-distribución) [6], the distribution system operator for the entirety of the distribution system in Tenerife, provided a satellite image of the 500m radius area around the EMMA, with markings according to the location of the different transformer stations, as shown in Figure 10. This image indicates that only a segment of the residential blocks at the north of the EMMA is supplied by the same transformer station, since an additional station is placed at the north-east.

The further clarification needed to correctly determine the residential blocks connected to the same transformer station as the EMMA is provided by the LV distribution grid map displayed in Figure 11, submitted once more by e-distribución [6].

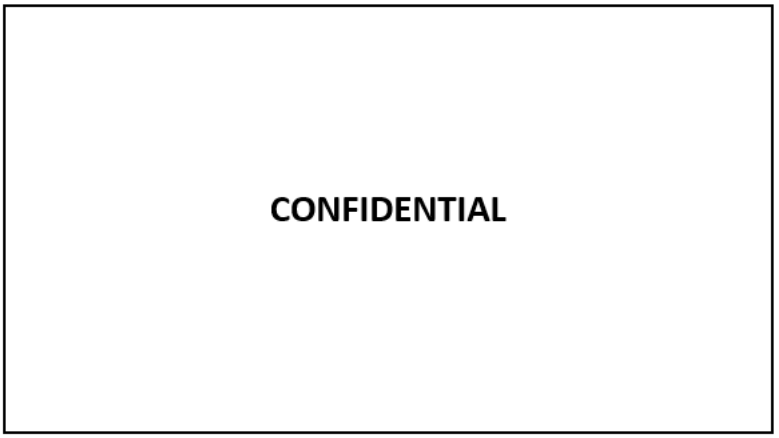

Figure 11: Analysed distribution grid connected to the EMMA, obtained from *e-distribución* [6].

Finally, combining the information extracted from Figures 9, 10 and 11, it can be established that the transformer station connected to the EMMA supplies the majority of the residential blocks at the north-north-east. However, the two building blocks in the northern limit as well as the block in the eastern limit, including half of the next building seem to be supplied by the transformer station at the east. Thus, the LV distribution grid considered to be connected to the same station as the EMMA for the purpose of this work is comprised by the supply points marked in Figure 12.

3.1.2 Electrical parameters

Starting from the established grid topology, the LV grid was modelled in OpenDSS, configuring 66 supply points including the EMMA, as well as the 20kV/400V transformer station. The 20kV MV grid connected to the station was configured as a circuit represented by a Thévenin equivalent. This allows to represent a part of the electrical network as a 'black box' defined by a voltage source and a series connected equivalent resistance [38]. The transformer station's capacity was set at 600kVA, as is common in Tenerife, since the stations tend to be standardized. The corresponding electrical parameters, such as the connection type (delta-wye), the resistance and the reactance where derived from the European-LV-Test-Feeder example case, which contains common and representative values.

To model the three-phase 230/400V LV lines, a *Linecode* was established, to apply the same parameters for all network lines. The resistances and reactances were extrapolated from the European-LV-Test-Feeder. This example case presents ten linecodes with different parameters. Thus, as shown in Figure 41, an average

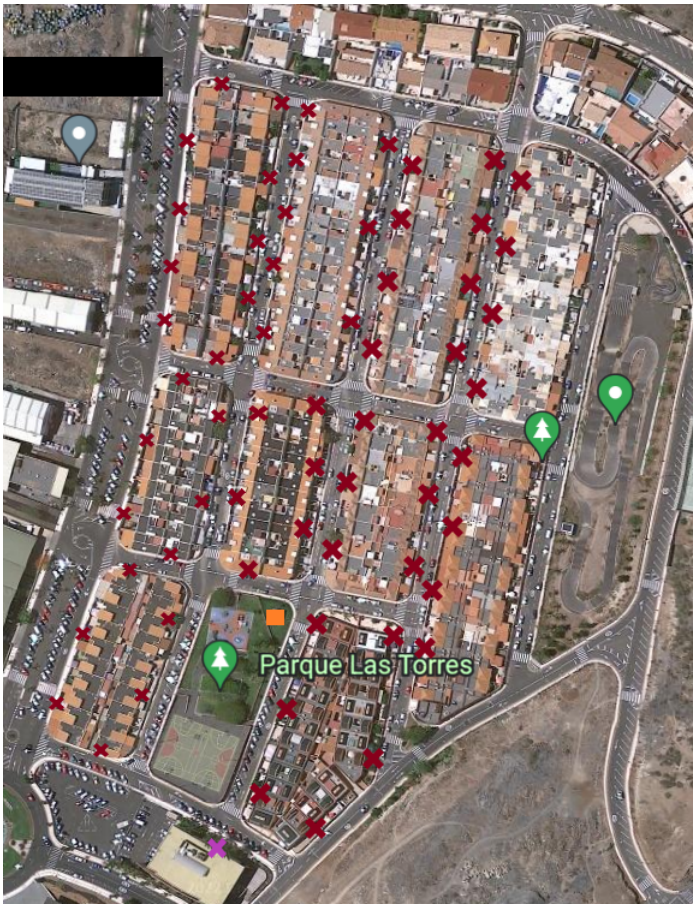

Figure 12: Supply points forming the LV grid analysed in this work.

value for each respective resistance and reactance was calculated, and input into the model as part of the linecode.

Furthermore, the lines were defined using satellite images from Google Maps to determine the geographical coordinates of the buses representing the supply points and overall grid topology, as well as the distances between them.

3.2 Loads

The spin-off from the University of La Laguna, Energy RIS [7], performed an analysis assessing the potential of Citizen Energy Communities in Tenerife, pointing to the municipality of Adeje as one of the best locations. For this analysis, Energy RIS took into consideration the number of dwellings and electric meters, as well as the available rooftop area for PV. More specifically, for the entirety of the residential blocks north-north-east of the EMMA shown in Figure 13, A total number of 432 electric meters and 290 dwellings was determined.

However, the LV grid connected to the same transformer station as the EMMA and studied in this work does not include the totality of the building blocks in the

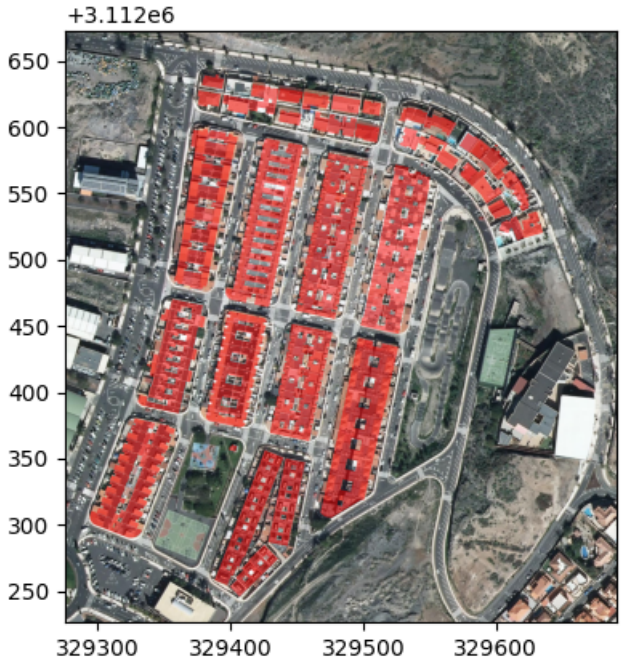

Figure 13: Entirety of the residential blocks north of the EMMA studied by Energy RIS [7].

area. Instead, around 25% of the dwelling area (the two blocks limiting to the north and half of the two blocks limiting to the east) is connected to a different transformer station located in the east. Thus, the effective values relevant for this work were reduced to 75% of the resulting numbers from Energy RIS' analysis, namely 324 electric meters and 216 dwellings, respectively.

The innovation project AdejeVerde, carried out jointly by Energy RIS and E.ON Innovation [39], connected neighbours from the 500m radius area of the EMMA to the 99kWp PV installation on the school's rooftop, creating the biggest energy community in Spain according to the number of participants. From said project, 53 real yearly residential consumption profiles were available for the area analysed in this work, in addition to weekly consumption profiles from the EMMA itself. In order to increase the number of profiles to 65 and match the number of consumption supply points determined in the previous section (excluding the transformer station), 11 additional profiles where estimated. For the first two profiles, the arithmetic mean and median of the available 53 real consumption profiles was calculated for each of the 8760 yearly hours. Figure 14 displays the resulting average profile, indicating that the mean hourly consumption tends to be between 150Wh and 700Wh, peaking at around 850Wh.

Next, each of the remaining 9 profiles was formed by the arithmetic mean of 5 different real consumption profiles. Finally, the available biweekly EMMA consumption profile shown in Figure 15 was replicated and expanded to cover the entirety

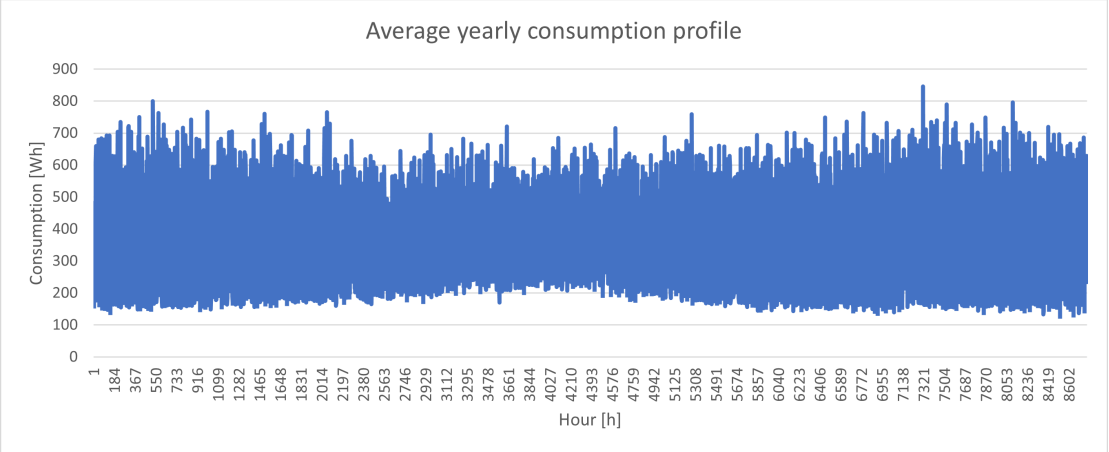

Figure 14: Average yearly residential consumption profile.

of the year. Taking into consideration previous yearly consumption values for 2017 and 2018, the estimated yearly consumption seems reasonable.

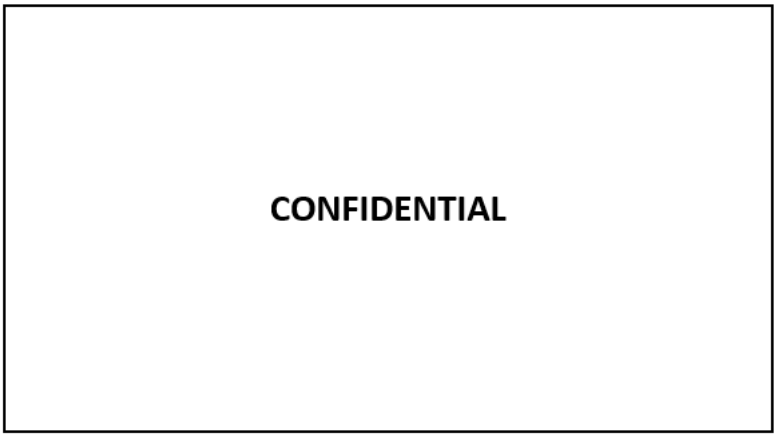

Figure 15: Biweekly EMMA consumption profile.

As a next step, the consumption simultaneity was considered. As previously stated, the analysed area consists of 324 residential electric meters, while 64 supply points are being configured in OpenDSS. Thus, each simulated supply point agglomerates 5 residential electric meters. According to the Decree 133/2011 of the Canary Islands [40], the distribution feeders needed to serve multiple supply points must be dimensioned for a load equal to the individual load multiplied by a simultaneity factor, defined in the low voltage electrotechnical regulation [34]. This regulation establishes a simultaneity factor of 4,6 for the agglomeration of 5 houses or supply points. Thus, each of the determined 64 consumption profiles is multiplied by said simultaneity factor (excluding the stand-alone EMMA consumption).

The resulting 65 consumption profiles were input into OpenDSS through the *Load* and *Loadshape* objects. To define the latter, each profile was normalized by dividing each value with the corresponding peak load. Then, they were uploaded as csv files. The loads were finally defined by the corresponding loadshape, the peak

load, voltage level and power factor, which according to the Decree 133/2011 of the Canary Islands [40] was set to 0,95 for calculation purposes.

3.3 PV systems

As explained in section 2.1, the main environmental factors influencing a PV system are the ambient temperature and solar irradiation. As such, a PV system is modelled in OpenDSS according to the following equations:

$$P_{PV} = P_p * T_{factor} * Ir_{factor} \tag{3}$$

$$P_{AC} = P_{PV} * \eta_{inverter} \tag{4}$$

The first equation indicates that the output PV power is calculated by multiplying the peak PV power with a temperature factor and an irradiation factor. The second shows that the PV system's output power is obtained by multiplying the previous result with the inverters's efficiency.

The corresponding meteorological parameters were extracted from the Photovoltaic Geographical Information System (PVGIS) version 5.2 [41]. It is a tool managed by the Joint Research Centre that uses satellite images as well as climate reanalysis models to calculate high-quality and high resolution meteorological data such as solar radiation, temperature and wind speed. The location of the EMMA was selected (28.125N, -16.737W) and data for a typical meteorological year (TMY) was requested. A TMY contains hourly data for a whole year. However, each month in the dataset is selected according to the most representative or typical year for that month, based on air temperature, global horizontal irradiance and relative humidity (Figure 42). This methodology follows the international Standard ISO 15927-4.

To apply these parameters to the PV model, a typical PV module was used as a reference, namely the Canadian Solar CS1H series [42] with a temperature coefficient of $-0.37\%/°C$. OpenDSS represents the temperature effects on PV system's performance through a definable Power-Temperature Curve. In this case, the temperature coefficient was used to define the curve, displayed in Figure 16. The temperature factor is then estimated based on this curve and the PV module temperature, which is calculated according to the next equation, where NOCT means normal operating cell temperature, that being $45°C$ at $20°C$ ambient temperature and $800W/m^2$ solar irradiation.

$$T_{cell} = T_{ambient} + G * \frac{NOCT - 20°C}{800W/m^2} \tag{5}$$

Furthermore, the irradiation-power curve is assumed to have a one-to-one correlation in OpenDSS. As such, for the irradiation factor definition, only the normalized irradiation values are required. However, reflection effects were additionally taken

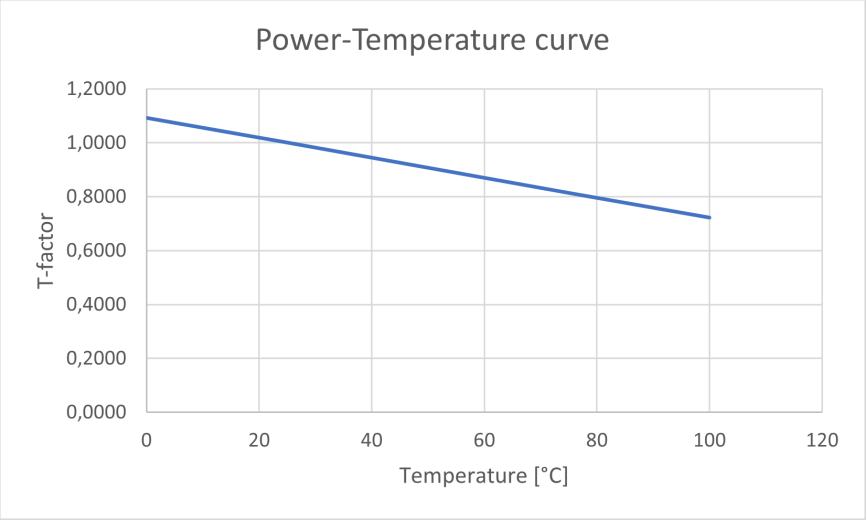

Figure 16: Power-Temperature curve.

Month	Fixed System	Azimuthal Tracking	Polar Tracking	Double Axis Tracking
January	0.948	0.988	0.992	1.000
February	0.926	0.989	0.994	1.000
March	0.913	0.991	1.000	1.000
April	0.898	0.993	0.993	1.000
May	0.914	0.994	0.982	1.000
June	0.886	0.994	0.989	1.000
July	0.883	0.993	0.991	1.000
August	0.902	0.993	0.989	1.000
September	0.887	0.991	0.999	1.000
October	0.934	0.990	0.997	1.000
November	0.937	0.987	0.992	1.000
December	0.944	0.986	0.990	1.000

Figure 17: Typical PV-Fresnell performance factors for the Canary Islands.

into consideration, represented by the Fresnell performance factors, whose typical values for the Canary Islands are listed in Figure 17.

Moreover, the inverter efficiency is also modelled through a definable Inverter-Efficiency Curve. For this matter, the STP 50-40 [43] curve shown in Figure 18 was applied as a reference.

Finally, the PV systems are modelled as three-phase systems connected to the 400V grid at the different supply points with a power factor of 1 and the corresponding temperature and irradiance values and defining curves.

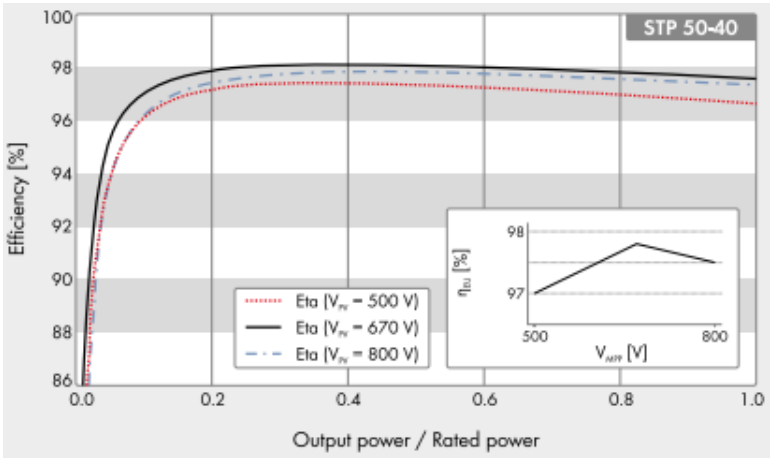

Figure 18: Typical inverter efficiency curve.

3.4 Simulation procedure

The simulation will be performed in three steps. In the first one, the residential network devoid of PV systems will be simulated, and adjusted accordingly if needed. For this matter, an OpenDSS object called *Monitor* will be set at different network points to study the yearly power and voltage profiles. Furthermore, an object called *Energymeter* will be configured at the transformer station to observe the voltage-over-distance profiles. In this step, the system will consist of the transformer station, connecting lines and 65 supply points only representing the residential loads.

In the second step, the PV systems will be implemented equally distributed among the analysed system, limited by the current Spanish regulation. The EMMA will have 99kWp PV system, while the remaining 64 supply points will be connected each to a 5kWp system, due to the regulatory limit in the Circular Letter 1/2021 [36]: the ratio of total injected DG power must be below 70% of the transformer station capacity.

In the last step, the maximum PV potential will be studied. For this purpose, the results obtained from Energy RIS' analysis will be applied. The total residential blocks area was estimated to have an available PV suited rooftop area of $16.104m^2$, so that the analysed area in this work (75% of the total) would correspond to $12.078m^2$. Then, a factor of $0,145kWp/m^2$ is applied, resulting in 1751,31kWp total installed residential PV capacity or 27,36kWp per supply point. A rather conservative factor is used to avoid overstatements, in the literature [44] uses $0,1875Wp/m^2$, while [32] consciously applies an over-conservative $0,143Wp/m^2$ to also account for service paths.

4 Results

4.1 Base Case

The analysed LV network was successfully implemented in OpenDSS. Its topology is shown in Figure 19, which matches the proposed system in Figure 12. In the first step, the current grid was modelled as the base case without integrating any PV systems. The corresponding voltage profile for a summer day is displayed in Figure 20. The per unit line-to-neutral voltage is represented with increasing distance from the transformer station. Additionally, the different branches of the radial distribution grid can be appreciated. As expected, with increasing distance, the voltage drops gradually. The most affected branches are the ones located at the north-east. In fact, the highest voltage drop is experienced in the farthest line, that being the one connecting the supply points located at the north-east limit.

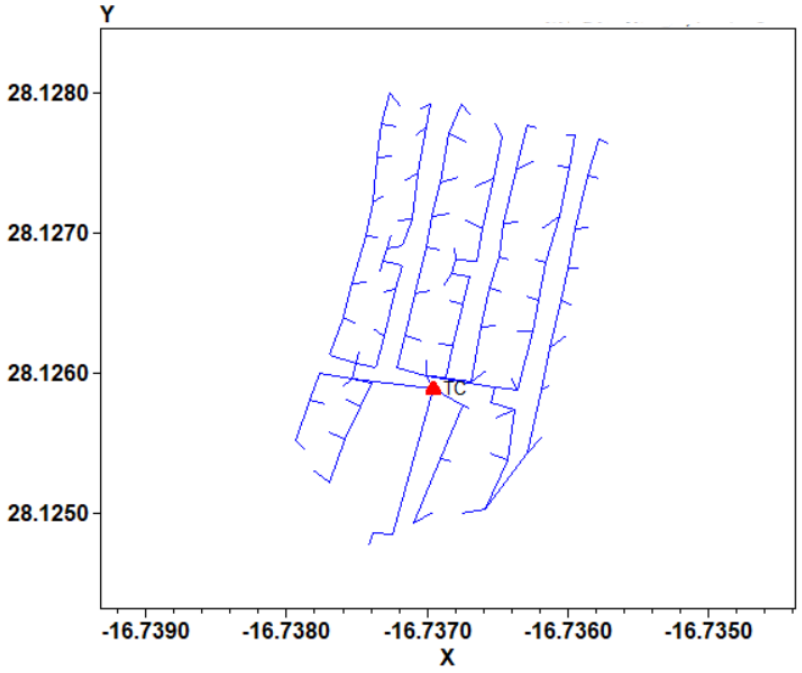

Figure 19: Analysed network in OpenDSS.

Thus, the yearly voltage profile at this critical point in the network is observed in more concrete terms. In fact, it is found out that the voltage exceeds the grid limits established by the European Standard EN 50160 of 230V +/- 10%, since at a certain time of the year the voltage drops below 206V, as shown in Figure 21. This critical result, however, is only found at this position in the network, since all other lines remain within statutory limits, as displayed in the yearly voltage profile of a line directly connected to the station in Figure 22.

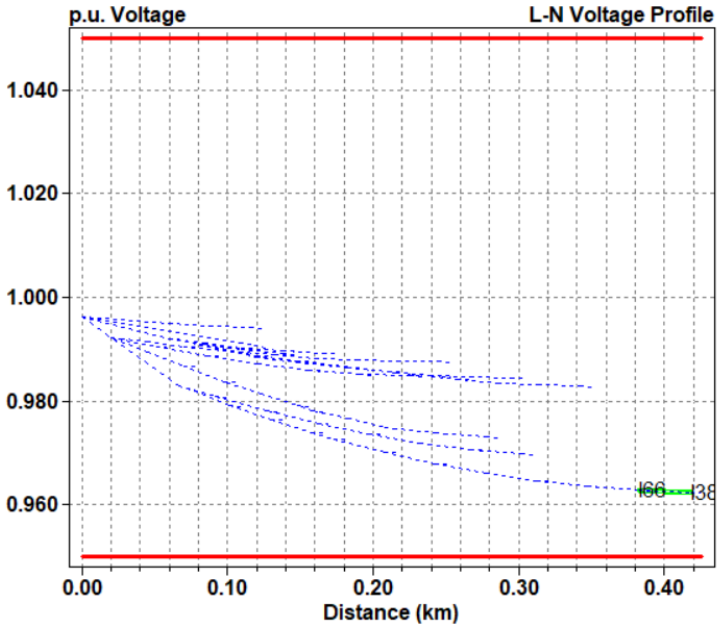

Figure 20: Typical voltage profile without PV Systems.

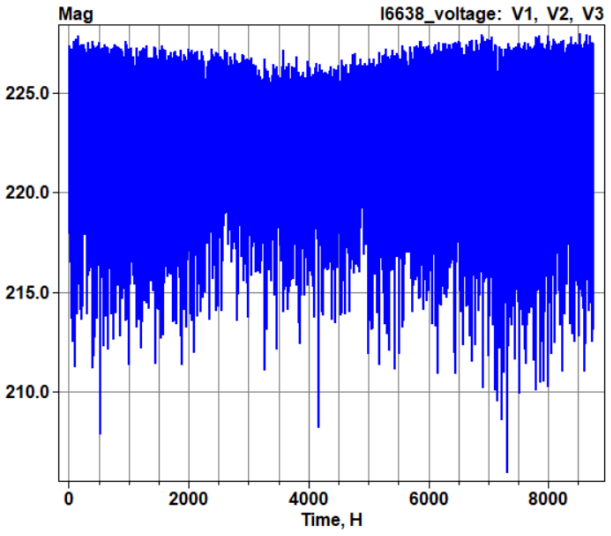

Figure 21: Yearly voltage profile at the farthest network line.

To solve this issue, a capacitor bank was modelled at the transformer station, to raise the voltage profiles and allow the network to comply with the grid regulation. The capacitor bank parameters were based on the EPRI Ckt-5 test circuit. It was connected in wye to the transformer station bus, and its capacity was set at 300kVar. As seen in Figure 24 and as a comparison to Figure 23, both representing an autumn evening with high consumption and thus, a high voltage drop, this capacitor increases the network voltage profile by around 2%. As a result, the yearly voltage profile of the previously critical line now complies with the European Standard EN 50160, as demonstrated by Figure 25, in comparison to the previous Figure 21. The lowest voltage now stays above 210V line-to-neutral voltage (8,7% deviation). Moreover,

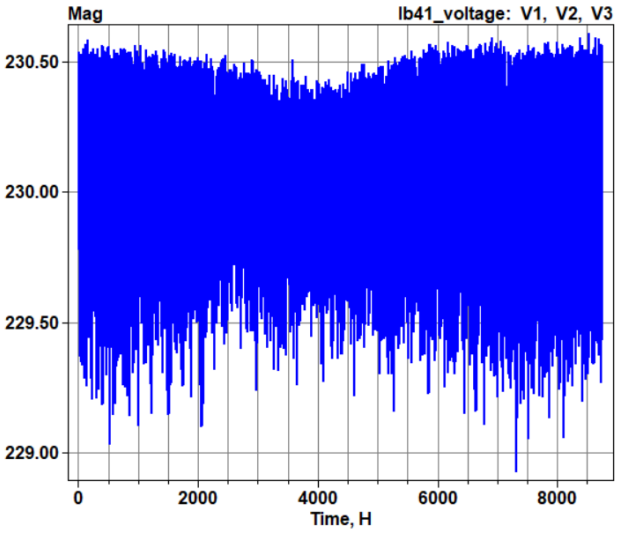

Figure 22: Yearly voltage profile at a line directly connected to the transformer station.

it is verified that after the implementation of the capacitor bank, the lines sourcing from the transformer station do not exceed the upper voltage limits. Indeed, Figure 26, as a contrast to Figure 22, shows that the integration of the capacitor bank causes the closest line to reach a voltage peak around 235,2V line-neutral voltage, complying with EN 50160 with only a 2,17% deviation.

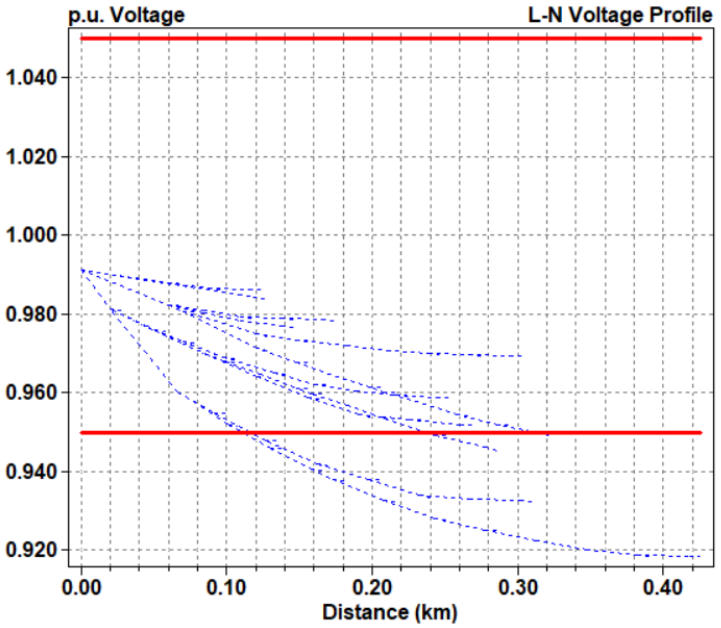

Figure 23: Critical voltage profile without a capacitor bank.

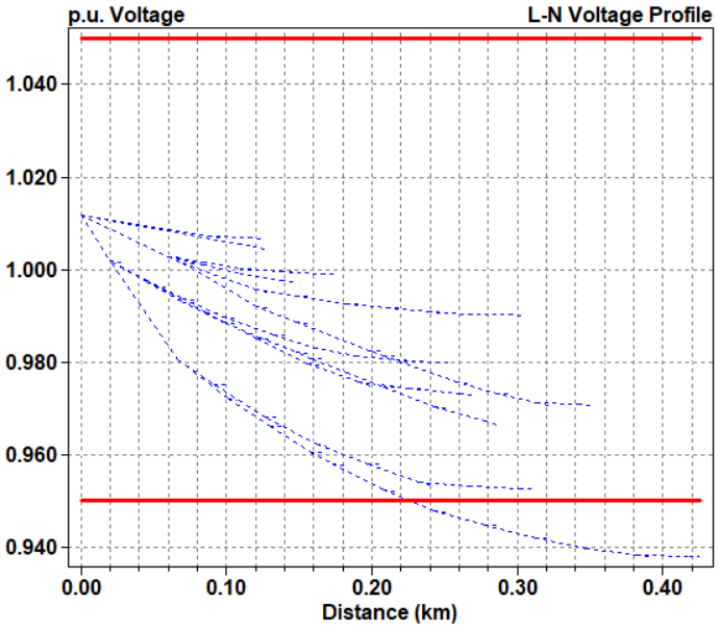

Figure 24: Critical voltage profile with a capacitor bank.

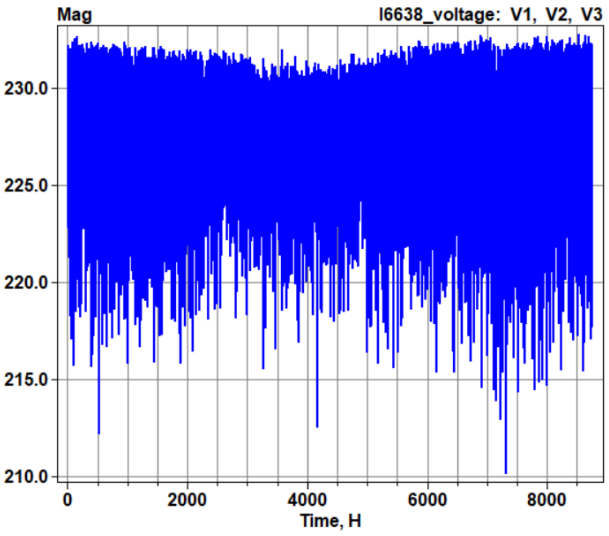

Figure 25: Yearly voltage profile at the farthest network line, after a capacitor has been included in the model.

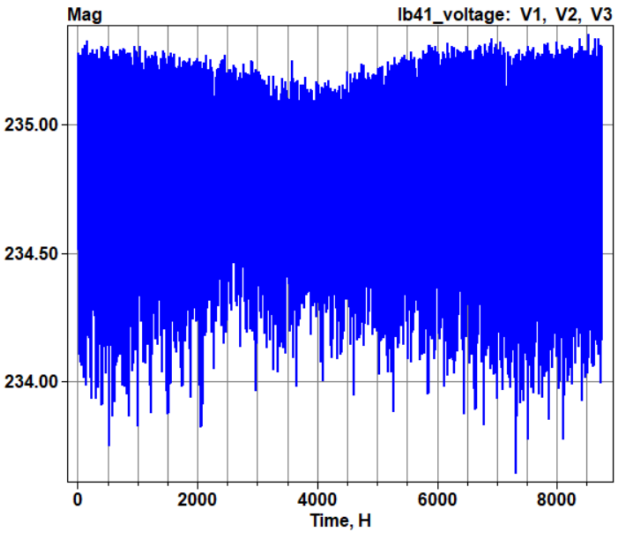

Figure 26: Yearly voltage profile at a line directly connected to the transformer station, after a capacitor has been included in the model.

4.2 Regulatory PV limits

As a next step, the PV system model was integrated into the simulation. To comply with the regulation limits stated in [36], the installed PV power for all residential supply points was set to 5kWp. Except for the PV installation in the EMMA rooftop of 99kWp, all other PV installations were integrated in an evenly distributed manner matching the supply points in Figure 12 and with the same installed power.

To verify the impact on the LV grid, a monitor was configured at the end of each feeder, as well as one next to the transformer station. By verifying the yearly voltage profile on each feeder, it can be noted that the regulatory limits of EN 50160 are respected in the whole network. However, an overall increase in the voltage profile and voltage deviation can be found, as clearly shown in Figure 27, representing the distance-voltage profile for a summer day with high PV yield. While all feeders experience a noticeable voltage increase in comparison to Figure 20, the EMMA feeder shows the highest voltage deviation by far. In fact, analysing the yearly power-flow at the EMMA supply point (Figure 28) shows that, except during the night, the PV production at the EMMA always surpasses consumption, leading to high grid power injection values.

In contrast, the residential supply points show a generally higher grid consumption than injection, as seen in Figure 29 for the farthest supply point. Moreover, while this point still shows the same lowest voltage value during the yearly profile, since it corresponds to a night value, the PV generation causes an increase in the maximum existing voltage values, as shown in Figure 30. In fact, this point shows one of the highest peak voltages, almost reaching 245V. Supply points closer to the transformer station show lower but still recognizable voltage increases, as it can be appreciated contrasting Figures 26 and 31. The voltage increment is especially no-

ticeable for the spring and summer months, represented in the middle section of the profiles.

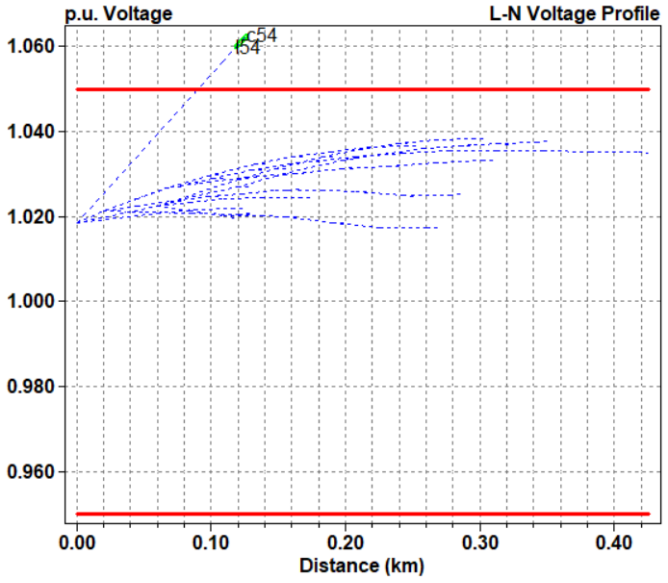

Figure 27: Distance-voltage profile for a summer day after the implementation of the PV systems.

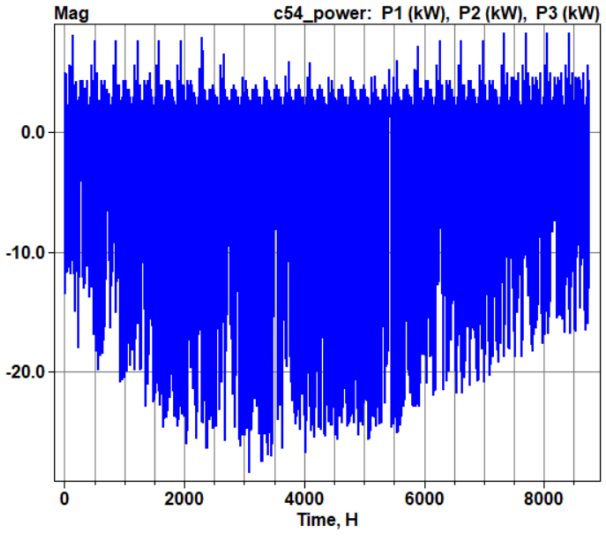

Figure 28: Yearly power-flow at the EMMA supply point after the implementation of the PV systems.

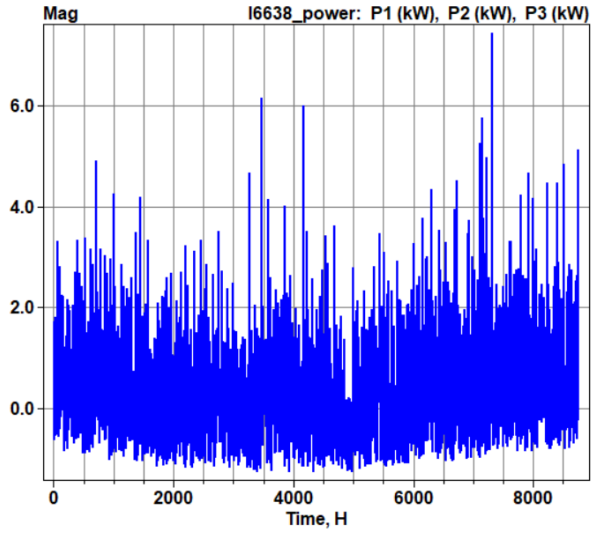

Figure 29: Yearly power-flow at the farthest supply point after the implementation of the PV systems.

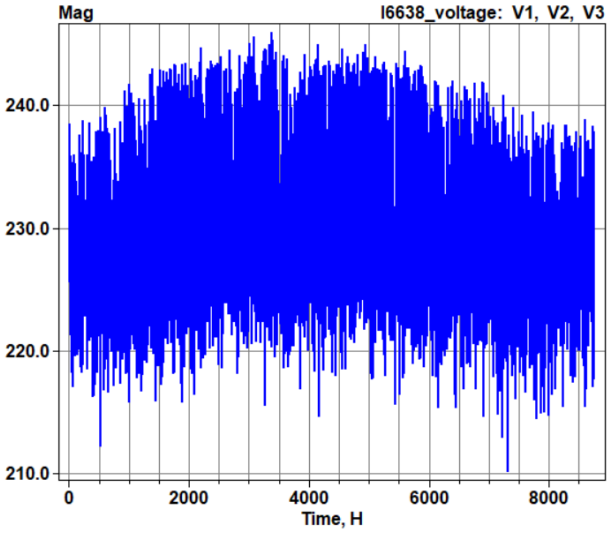

Figure 30: Yearly voltage profile at the farthest point after the implementation of the PV systems.

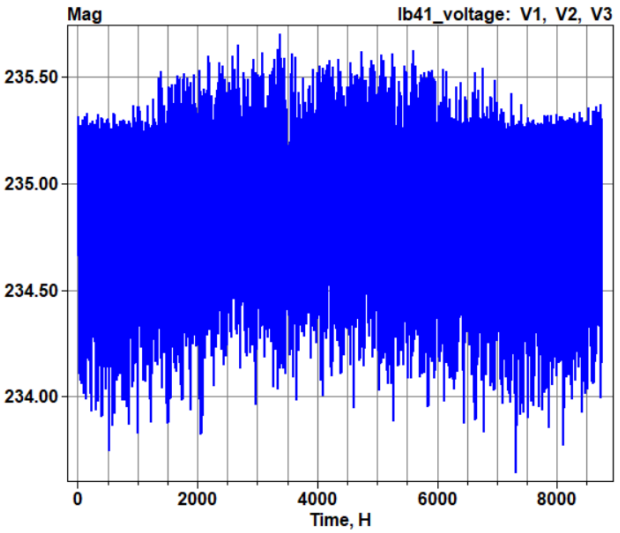

Figure 31: Yearly voltage profile at a line directly connected to the transformer station after the implementation of the PV systems.

However, the highest voltage deviation in the network is found at the EMMA supply point, as stated previously, which can be recognized in Figure 32. This is caused by the 99kWp PV installation, which remarkably surpasses all other individual PV installations. This supply point will in fact consistently exceed the 230V nominal line-to-neutral voltage and even reach values around 245,3V, approximately 12,5V higher than its PV devoid profile. This represents a 5,43% voltage deviation in the LV grid caused by a single DG, which would not comply with the Royal Decree 1699/2011 [35], exceeding the limit of 2,5%. This means that according to real time network operations, the EMMA PV generation may need to be partially curtailed.

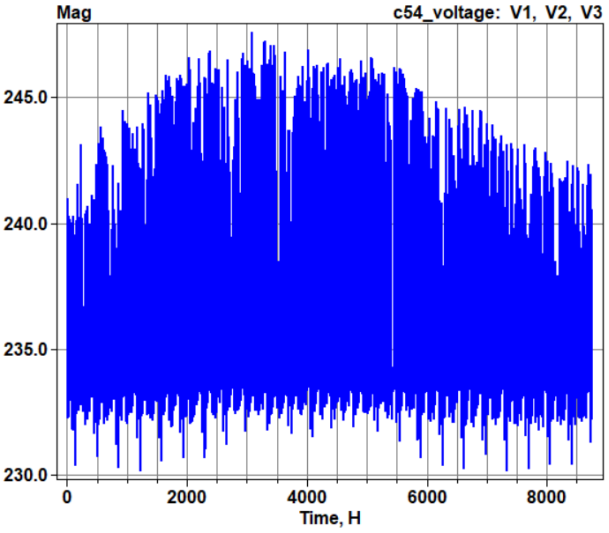

Figure 32: Yearly voltage profile at the EMMA after the implementation of the PV systems.

4.3 Maximum PV potential

In this last step, firstly, the maximum installable PV capacity according to available rooftop area was implemented in the simulation, that being 27,36kWp per residential supply point, in addition to the EMMA 99kWp. Then, the impact on the LV network was analysed.

Figure 33 distinctly illustrates the remarkable increase in the voltage profile, caused by multiplying the residential installed PV capacity by more than 5. The majority of feeders are now breaching the limits stipulated by EN 50160. In fact, it can be noticed that the farthest feeder experiences the most critical voltage deviation, surpassing 1,35pu. On the contrary, the EMMA supply point experienced the least variation from the previous case. The power-flow as well as the voltage profiles remained nearly unchanged. The network points located near the transformer station show the least voltage increase, usually still within limits, the line displayed in Figure 34 reaches a maximum deviation of around 3%. Despite this, the farthest point suffers the highest voltage deviation as shown in Figure 35, reaching extreme values above 340V, almost 48% above nominal voltage.

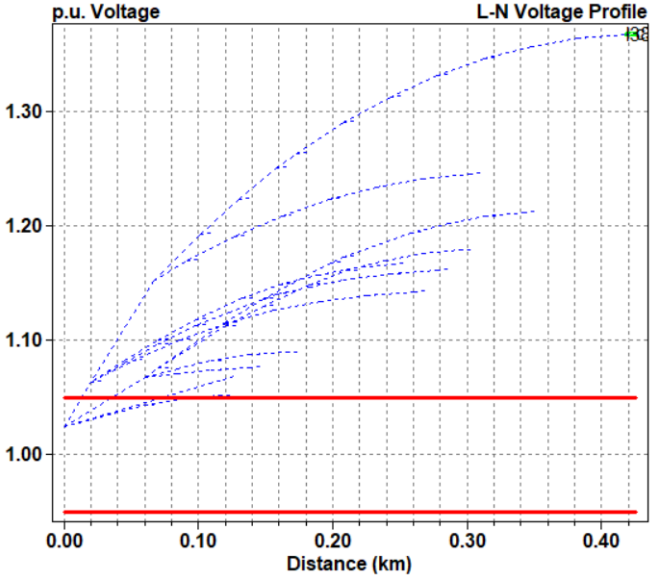

Figure 33: Distance-voltage profile for a summer day after the implementation of the maximum potential PV capacity.

The farthest network point shows a noticeable change in its power-flow as well, as illustrated in Figure 36. This stands out when contrasted with Figure 29, since the grid injection now prevails over the consumption for the supply point. Moreover, while the voltage deviation is considerably less severe, the change in the power-flow profile is more extreme the closer to the transformer station. The supply point at the line directly connected to the station now shows a power-flow profile similar to the EMMA in Figure 28.

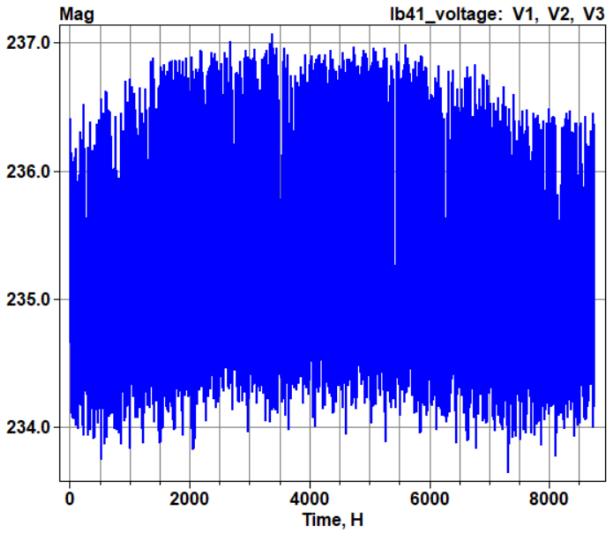

Figure 34: Yearly voltage profile at a line directly connected to the transformer station point after the implementation of the maximum PV potential.

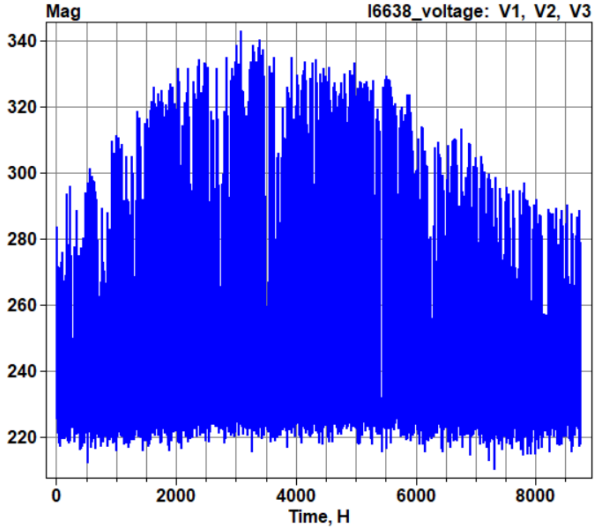

Figure 35: Yearly voltage profile at the farthest point after the implementation of the maximum PV potential.

The most drastic change in power-flow profile is illustrated in Figures 37 and 38. While the first yearly profile shows a power-flow sourcing from the transformer station and feeding the network lines, with positive power values throughout the whole year, the latter clearly illustrates the reverse power-flow caused by the PV generation. While this line still shows positive, station-to-feeder flow values for the nighttime hours, for the daytime hours, and especially during spring and summer, the reverse power-flow is up to 5 times higher than the station-to-feeder flow. Despite this result, the voltage profile at this line does not breach the limits, as seen in Figure 39, the maximum voltage deviation stays below 2,4% of the nominal voltage.

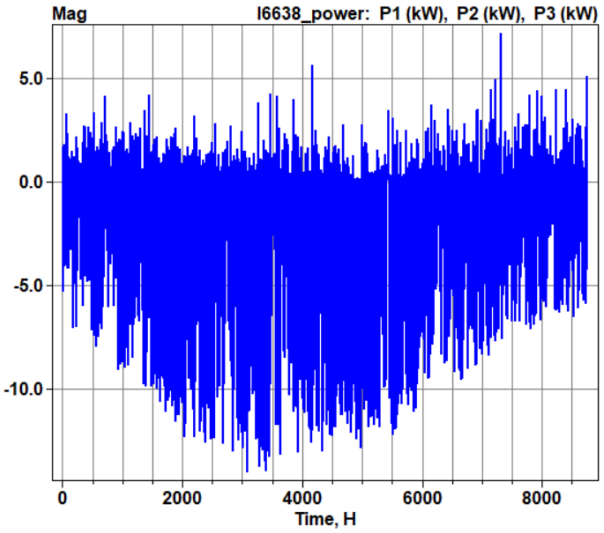

Figure 36: Yearly power-flow at the farthest supply point after the implementation of the maximum PV potential.

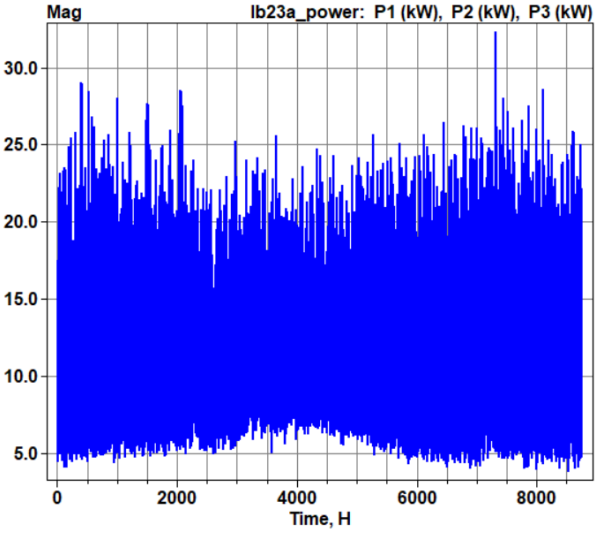

Figure 37: Yearly power-flow at one of the main lines emerging from the transformer station, before the implementation of the maximum PV potential.

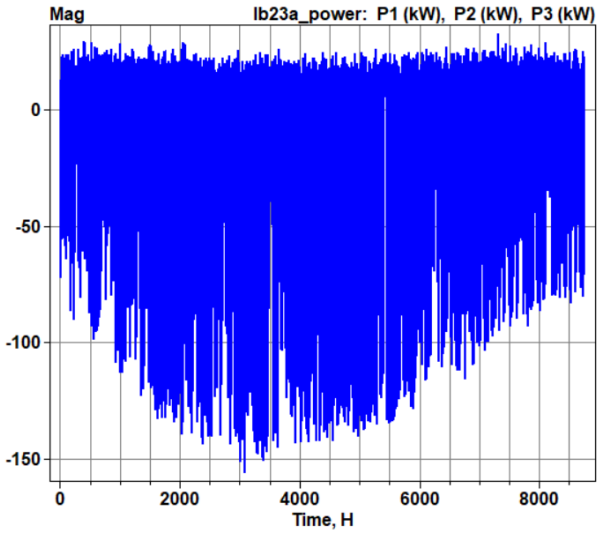

Figure 38: Yearly power-flow at one of the main lines emerging from the transformer station, after the implementation of the maximum PV potential.

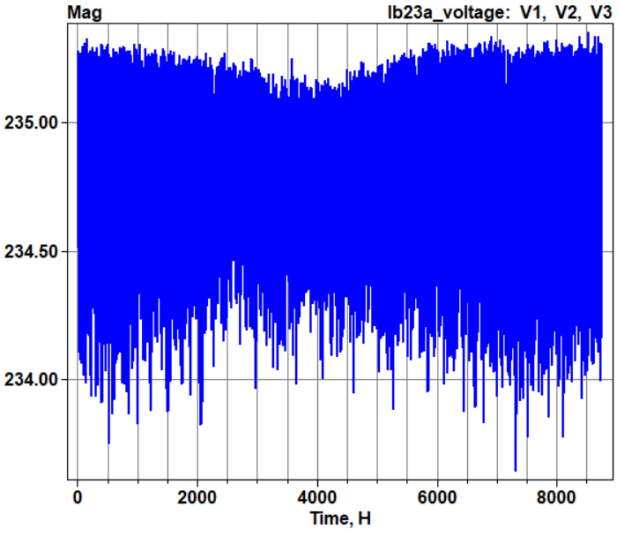

Figure 39: Yearly voltage profile at one of the main lines emerging from the transformer station, after the implementation of the maximum PV potential.

5 Discussion

The simulation results show that a scenario with evenly distributed residential PV systems in the analysed LV grid limited by the 70% of the transformer station capacity [36] would also comply with voltage limits, thus justifying its feasibility. However, this case implies the installation of just 320kWp of rooftop PV, in addition to the EMMA 99kWp. Although the PV potential of this area, according to available rooftop area, is much higher, namely by a factor of 5,47, this maximum potential scenario would breach the voltage limits of EN 50160. Despite this, if the regulation restriction in [36] is not taken into consideration, it is possible to increase the installed PV capacity up to around 7,5kWp per supply point, for a total of 480kWp, 579kWp with the EMMA. This value sets the limit so that the farthest feeder complies with the maximum 10% voltage deviation, as seen in Figure 40. This could however exceed the feeder capacity.

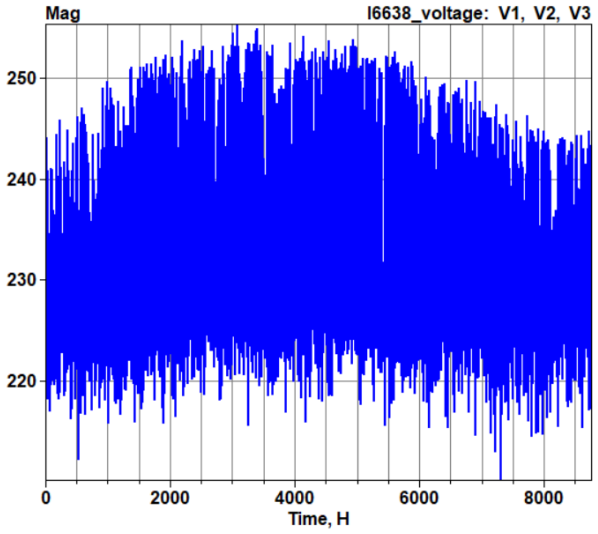

Figure 40: Yearly voltage profile at the farthest network line, for a 7,5kWp PV installation per residential supply point.

In relation to this, as illustrated in Figure 38, the critically high reversed power-flow found at lines near the transformer station would put the network components at risk of exceeding thermal limits due to the extreme current flows. To further analyse this limiting factor, more information regarding conductor parameters and overall capacity would be required.

It is noteworthy to state that the simulation results demonstrate the statements found in the literature. The different yearly voltage profiles clearly show the relations stated in Equation 1 and Figure 6. While the residential loads caused a sheer voltage drop, increasing with line distance, the introduced capacitor bank was able to increase the voltage level, and the distributed generation from PV systems further increased the voltage. Furthermore, as mentioned in the studies [27],[28],[3] and [29], the location of the PV system in relation to the transformer station was proven to play a crucial role. As already appreciated in Figures 29 and 31, the longer the

distance, the higher the voltage deviation, while points near the station suffer from higher power-flows. However, in contrast to these sources, the first limiting factor in the performed simulation was found to be the grid/station capacity of [36], since the voltage deviation limit of EN 50160 was reached at a higher PV penetration. Despite this, the voltage deviation limit was reached before the maximum rooftop potential, at a 38% higher PV penetration. In accordance with [31], the feeder length and impedance were demonstrated to be key factors affecting the voltage drop.

Finally, the statement found in [21] is further justified with these simulation results. While upgrades to the current grid infrastructure are needed to allow a higher PV penetration, the implementation of grid support techniques through smart inverters is essential. As such, the next step required to further analyse the potential PV penetration in a LV network is the implementation of the Volt-Var and Volt-Watt techniques found in Figure 7. These control techniques are only partially integrated into OpenDSS, and it would require an interface to an additional programming environment to define said techniques in accordance to the applicable regulation. In fact, while the grid codes in other countries such as Germany [2] and Australia [45] already define flexible power factors in LV grids to allow DG to offer ancillary services, in Spain [35] the DG power factor is limited to 0,98, restricting the implementation of said techniques. As such, modifications in the current regulation would be needed. However, a potential solution is being researched in the energy innovation domain, with the integration of distribution static synchronous compensators, which would be able to integrate the control properties of solar inverters, voltage regulators, power factor correction and energy storage. This device is able to absorb and inject both active and reactive power at full rating and arises as a solution to regulatory power factor limits, since they can be coupled with a solar inverter so that the inverter works at a unity power factor while the distribution static synchronous compensator provides the necessary reactive power, allowing the PV system to provide higher power outputs while providing grid voltage control. Also, an optimally placed device would avoid the inequity found in Volt-Watt and Volt-Var control schemes, where the systems at the feeder's end need to supply more reactive power.

6 Conclusion

This work determines the limits to the rooftop PV penetration in a real case scenario, a distribution network in the municipality of Adeje, Tenerife, Spain. The LV distribution grid connected to the same transformer station as the EMMA was simulated in OpenDSS. The model was programmed integrating real network topology information, as well as real consumption data, coupled with typical and representative electrical parameters. The current Spanish grid regulation was followed to determine the statutory limits for rooftop PV penetration. After successfully modelling the LV network represented by 65 supply points and a transformer station, it was found out that by applying the limit of 70% of the transformer station capacity to the total injected PV power, the voltage was kept within the permissible range. While this restriction would allow to install a total of 420kWp, this value could be increased up to around 579kWp until the voltage limits are breached. By means of the simulation results, the impact of the distributed PV generation, as well as the location of the supply point to the transformer station on the grid voltage and power-flow were demonstrated. Furthermore, using the available rooftop area to determine the maximum PV potential in the area granted a PV capacity of around 1859,21kWp. However, this scenario greatly surpassed the statutory voltage and capacity limits.

As a potential solution for a higher PV penetration complying with grid limitations, the Volt-Var and Volt-Watt techniques are discussed. However, the implementation of said techniques may require to adapt current grid regulation, as would be the case in Spain. Thus, this work points towards the implementation analysis of these techniques, and its comparison with other energy innovation solutions such as distribution static synchronous compensators, as future lines of research.

Acknowledgements

I would like to sincerely thank Professor Ricardo Guerrero for tutoring this Master thesis and guiding me with interesting insights and useful advice. Furthermore, I would also like to thank Jose Manuel Valle from Endesa for the provided information which was a fundamental part of this work, as well as Professor Felipe Monzon. Moreover, I sincerely thank Luis Hernandez and Inigo Berazaluce, as well as my other E.ON Innovation colleagues for the opportunity given to me to participate in this challenging and inspiring project and for supporting me with the thesis. I am as well grateful to David Cañadillas from EnergyRIS for the valuable information shared with me. Finally, I would like to say a big thank you to my family and friends who have supported me all along.

References

[1] International Renewable Energy Agency, "World Energy Transitions Outlook 2022." https://www.irena.org/publications/2022/Mar/World-Energy-Transitions-Outlook-2022, Mar 2022. [Online; accessed 02-August-2022].

[2] IEA, "Do It Locally: Local Voltage Support by Distributed Generation – A Management Summary." https://iea-pvps.org/wp-content/uploads/2020/01/Task_14_Report__Do_It_Locally_IEA_Final_T14.08.pdf, Jan 2017.

[3] I. A. Ibrahim and M. J. Hossain, "A benchmark model for low voltage distribution networks with pv systems and smart inverter control techniques," *Renewable and Sustainable Energy Reviews*, vol. 166, 2022.

[4] N. Tyutyundzhiev, K. Lovchinov, H. Nichev, and M. Petrov, "Open dss simulations of power fluctuations induced by rooftop pv generator on a building lv electrical grid," *Journal of Multidisciplinary Engineering Science and Technology*, vol. 3, pp. 2458–9403, 12 2016.

[5] "Inkolan." https://www.inkolan.com/. [Accessed Aug 2022].

[6] "EDISTRIBUCIÓN Redes Digitales, S.L.U.." https://www.edistribucion.com/es/index.html. [Accessed Aug 2022].

[7] "Energy RIS - Energy Research and Intelligence Solutions." http://energyris.com/. [Accessed Aug 2022].

[8] "Real Decreto 568/2022, de 11 de julio, por el que se establece el marco general del banco de pruebas regulatorio para el fomento de la investigación y la innovación en el sector eléctrico." https://www.boe.es/eli/es/rd/2022/07/11/568, Jul 2022. [Reference code: BOE-A-2022-11511].

[9] "National Integrated Energy and Climate Plan (PNIEC) 2021 2030." https://www.boe.es/boe/dias/2021/03/31/pdfs/BOE-A-2021-5106.pdf, Mar 2021.

[10] International Renewable Energy Agency, "Future of Solar Photovoltaic." https://irena.org/-/media/Files/IRENA/Agency/Publication/2019/Nov/IRENA_Future_of_Solar_PV_2019.pdf, Nov 2019. [Online; accessed 02-August-2022].

[11] E. Hartvigsson, M. Odenberger, P. Chen, and E. Nyholm, "Estimating national and local low-voltage grid capacity for residential solar photovoltaic in sweden, uk and germany," *Renewable Energy*, vol. 171, pp. 915–926, 2021.

[12] "Real Decreto 244/2019, de 5 de abril, por el que se regulan las condiciones administrativas, técnicas y económicas del autoconsumo de energía eléctrica." https://www.boe.es/eli/es/rd/2019/04/05/244, Apr 2019. [Reference code: BOE-A-2019-5089].

[13] International Energy Agency, "Net Zero by 2050: A Roadmap for the Global Energy Sector." https://iea.blob.core.windows.net/assets/deebef5d-0c34-4539-9d0c-10b13d840027/NetZeroby2050-ARoadmapfortheGlobalEnergySector_CORR.pdf, May 2021. [Online; accessed 08-August-2022].

[14] Australian Energy Regulator, "Wholesale markets quarterly - Q4 2021." https://www.aer.gov.au/wholesale-markets/performance-reporting/wholesale-markets-quarterly-q4-2021, Feb 2022. [Online; accessed 18-August-2022].

[15] Tim Sylvia, "Hawaiian Electric saw a 55% increase in home solar installations in 2020." https://pv-magazine-usa.com/2021/01/27/hawaiian-electric-saw-a-55-increase-in-home-solar-installations\-in-2020/, Jan 2021. [Online; accessed 30-June-2022].

[16] "Directive (EU) 2018/2001 of the European Parliament and of the Council of 11 December 2018 on the promotion of the use of energy from renewable sources." http://data.europa.eu/eli/dir/2018/2001/oj, Dec 2018. [Reference code: PE/48/2018/REV/1].

[17] "Directive (EU) 2019/944 of the European Parliament and of the Council of 5 June 2019 on common rules for the internal market for electricity and amending Directive 2012/27/EU." ttp://data.europa.eu/eli/dir/2019/944/oj, Jun 2019. [Reference code: PE/10/2019/REV/1].

[18] A. Caramizaru, A. Uihlein, and E. C. J. R. Centre, *Energy Communities: An Overview of Energy and Social Innovation*. EUR (Luxembourg. Online), Publications Office of the European Union, 2020.

[19] Diario de Avisos, "Canarias debe aprovechar los fondos europeos para el despliegue renovable." https://diariodeavisos.elespanol.com/2022/06/canarias-fondos-europeos/, Jun 2022. [Online; accessed 6-July-2022].

[20] R. Tonkoski, L. A. C. Lopes, and T. H. M. El-Fouly, "Coordinated active power curtailment of grid connected pv inverters for overvoltage prevention," *IEEE Transactions on Sustainable Energy*, vol. 2, no. 2, pp. 139–147, 2011.

[21] K. Bódis, I. Kougias, A. Jäger-Waldau, N. Taylor, and S. Szabó, "A high-resolution geospatial assessment of the rooftop solar photovoltaic potential in the european union," *Renewable and Sustainable Energy Reviews*, vol. 114, 2019.

[22] E. Zio, M. Delfanti, L. Giorgi, V. Olivieri, and G. Sansavini, "Monte carlo simulation-based probabilistic assessment of dg penetration in medium voltage distribution networks," *International Journal of Electrical Power and Energy Systems*, vol. 64, pp. 852–860, 2015.

[23] I. Abdelmotteleb, T. Gómez, and J. P. Chaves-Avila, "Benefits of pv inverter volt-var control on distribution network operation," in *2017 IEEE Manchester PowerTech*, pp. 1–6, 2017.

[24] A. Samadi, R. Eriksson, L. Söder, B. G. Rawn, and J. C. Boemer, "Coordinated active power-dependent voltage regulation in distribution grids with pv systems," *IEEE Transactions on Power Delivery*, vol. 29, no. 3, pp. 1454–1464, 2014.

[25] Y. Yang, P. Enjeti, F. Blaabjerg, and H. Wang, "Wide-scale adoption of photovoltaic energy: Grid code modifications are explored in the distribution grid," *IEEE Industry Applications Magazine*, vol. 21, no. 5, pp. 21–31, 2015.

[26] W. Nacmanson and L. Ochoa, "Advanced Planning of PV-Rich Distribution Networks Deliverable 6: Consolidation of Findings (Final Report)." https://arena.gov.au/assets/2021/03/advanced-planning-of-pv-rich-distribution-network-deliverable-6.pdf, Feb 2021. [Online; accessed 12-August-2022].

[27] T. Aziz and N. Ketjoy, "Pv penetration limits in low voltage networks and voltage variations," *IEEE Access*, vol. 5, pp. 16784–16792, 2017.

[28] B. Bayer, P. Matschoss, H. Thomas, and A. Marian, "The german experience with integrating photovoltaic systems into the low-voltage grids," *Renewable Energy*, vol. 119, pp. 129–141, 2018.

[29] B. N. Jha and A. K. Mishra, "Maximum possibility of photovoltaic penetration in nepalese low voltage distribution network," in *Proceeding - ICERA 2021: 2021 3rd International Conference on Electronics Representation and Algorithm*, pp. 7–12, 2021.

[30] M. A. Eltawil and Z. Zhao, "Grid-connected photovoltaic power systems: Technical and potential problems-a review," *Renewable and Sustainable Energy Reviews*, vol. 14, no. 1, pp. 112–129, 2010.

[31] R. Tonkoski, D. Turcotte, and T. H. M. EL-Fouly, "Impact of high pv penetration on voltage profiles in residential neighborhoods," *IEEE Transactions on Sustainable Energy*, vol. 3, no. 3, pp. 518–527, 2012.

[32] Thomas Huld, Katalin Bodis, Irene Pinedo Pascua, Ewan Dunlop, Nigel Taylor, Arnulf Jäger-Waldau, "The Rooftop Potential For PV Systems In The European Union To Deliver The Paris Agreement." https://www.europeanenergyinnovation.eu/Articles/Spring-2018/The-Rooftop-Potential-for-PV-Systems-in-the-European-Union\-to-deliver-the-Paris-Agreement, 2018. [Online; accessed 18-August-2022].

[33] "Real Decreto-ley 6/2022, de 29 de marzo, por el que se adoptan medidas urgentes en el marco del Plan Nacional de respuesta a las consecuencias económicas y sociales de la guerra en Ucrania." https://www.boe.es/eli/es/rdl/2022/03/29/6, Mar 2022. [Reference code: BOE-A-2022-4972].

[34] "Reglamento electrotécnico para baja tensión e ITC." https://www.boe.es/biblioteca_juridica/codigos/codigo.php?modo=2&id=326_Reglamento_electrotecnico_para_baja_tension_e_ITC. [Updated March 2022].

[35] "Real Decreto 1699/2011, de 18 de noviembre, por el que se regula la conexión a red de instalaciones de producción de energía eléctrica de pequeña potencia." https://www.boe.es/eli/es/rd/2011/11/18/1699, Dec 2011. [Reference code: BOE-A-2011-19242].

[36] "Circular 1/2021, de 20 de enero, de la Comisión Nacional de los Mercados y la Competencia, por la que se establece la metodología y condiciones del acceso y de la conexión a las redes de transporte y distribución de las instalaciones de producción de energía eléctrica." https://www.boe.es/eli/es/cir/2021/01/20/1/con, Jan 2021. [Reference code: BOE-A-2021-904].

[37] Electric Power Research Institute, "Simulation Tool – OpenDSS." https://smartgrid.epri.com/SimulationTool.aspx. [Downloaded in https://sourceforge.net/projects/electricdss/].

[38] K. Moffat and A. Von Meier, "Linear quadratic phasor control of unbalanced distribution networks," in *2021 IEEE Madrid PowerTech, PowerTech 2021 - Conference Proceedings*, 2021.

[39] "E.ON Group Innovation GmbH." https://www.eon.com/en/innovation.html. [Accessed Aug 2022].

[40] "DECRETO 133/2011, de 17 de mayo, sobre el dimensionamiento de las acometidas eléctricas y las extensiones de redes de distribución en función de la previsión de carga simultánea." http://www.gobiernodecanarias.org/boc/2011/111/001.html, Jun 2011. [Reference code: BOC-A-2011-111-3086].

[41] E. Commission, "Photovoltaic Geographical Information System." https://re.jrc.ec.europa.eu/pvg_tools/en/. [Accessed Aug 2022].

[42] C. Solar, "Canadian Solar HiDM modules." https://www.canadiansolar.com/hidm/. [Accessed Aug 2022].

[43] SMA, "Sunny Tripower 50-40." https://files.sma.de/downloads/STP50-40-DS-de-30.pdf. [Accessed Aug 2022].

[44] R. Gupta, A. Pena-Bello, K. N. Streicher, C. Roduner, D. Thöni, M. K. Patel, and D. Parra, "Spatial analysis of distribution grid capacity and costs to enable massive deployment of pv, electric mobility and electric heating," *Applied Energy*, vol. 287, 2021.

[45] The Australian PV Association, "PV Integration on Australian distribution networks." https://apvi.org.au/wp-content/uploads/2013/12/APVA-PV-and-DNSP-Literature-review-September-2013.pdf, Sep 2013. [Online; accessed 18-August-2022].

A Annex

	R1	X1	R0	X0
1	3,97000	0,09900	3,97000	0,09900
2	1,25700	0,08500	1,25700	0,08500
3	1,15000	0,08800	1,20000	0,08800
4	0,86800	0,09200	0,76000	0,09200
5	0,46900	0,07500	1,58100	0,09100
6	0,27400	0,07300	0,95900	0,07900
7	0,08900	0,06750	0,31900	0,07600
8	0,16600	0,06800	0,58000	0,07800
9	0,44600	0,07100	1,50500	0,08300
10	0,32200	0,07400	0,80400	0,09300
AVG	**0,90110**	**0,07925**	**1,29350**	**0,08640**

Figure 41: Resistances and reactances from the European-LV-Test-Feeder, and the resulting averages, in Ohm/km.

month	year
1	2006
2	2007
3	2012
4	2011
5	2005
6	2009
7	2010
8	2009
9	2009
10	2005
11	2006
12	2010

Figure 42: Yearly datasets used to represent each month of the TMY.